Multimode interference devices for focusing in microfluidic channels

Hamish C. Hunt and James S. Wilkinson*

Optoelectronics Research Centre, University of Southampton, Southampton, SO17 1BJ, UK
**Corresponding author: jsw@orc.soton.ac.uk*

Low-cost, compact, automated optical microsystems for chemical analysis such as micro-flow cytometers for identification of individual biological cells require monolithically-integrated microlenses for focusing in microfluidic channels, to enable high-resolution scattering and fluorescence measurements. The multimode interference device (MMI), which makes use of self-imaging in multimode waveguides, is shown to be a simple and effective alternative to the microlens for microflow cytometry. MMIs were designed, realized and integrated with microfluidic channels in a silica-based glass waveguide material system. Focal spotsizes of 2.4 μm for MMIs have been measured at foci as far as 43.7 μm into the microfluidic channel.
OCIS Codes: 130.0130, 230.0230, 120.0120

The lab-on-a-chip offers great benefits for chemical and biochemical analysis in terms of reagent and sample consumption, speed, precision, and automation. Monolithic integration promises low cost and ease of use by non-experts, resulting in increasing adoption of microfluidic approaches for chemical analysis and in microflow cytometry in particular [1]. The use of light for detection of particles and chemical species within microfluidic systems is becoming widespread because of the sensitivity and specificity which can be achieved. Nonetheless, full integration of optical functions within microfluidic chips is in its infancy [2].

The integration of optical waveguides in planar microfluidic systems can exploit a common microfabrication technology [1] and brings advantages in terms of stability, robustness and sensitivity [3]. Integrated microlenses are required to focus light in the microfluidic channels where light diffracts freely. Approaches to miniaturizing macro-lenses described in the literature concentrate on the use of refractive lenses to improve fluorescence measurements. Such lenses have been shown to enhance performance [4] and reduction of aberrations has been achieved using compound lenses [5]. The performance of such unguided lens systems is limited by the high on-chip losses incurred through diffraction. Waveguiding lenses can be integrated into the waveguide system to minimise overall on-chip losses, additionally allowing realization of improved on-chip detection optics [6]. Planar fabrication technology allows straightforward replication of aspherical lenses so that a single lens rather than a compound system of lenses may be used to give good performance in a much more compact structure.

Diffractive lenses with kinoform profiles offering the greatest theoretical efficiency [7], have been realized and have achieved focusing in the centre of a microfluidic channel [8, 9]. However, the features of the ideal kinoform structure are too fine for high-quality replication by conventional photolithography. In this Letter, the design, fabrication and performance of a multimode interference device, or MMI, used to focus or image a spot into the middle of a microfluidic channel is described, exemplifying an alternative approach to imaging.

An MMI comprises one or more single mode waveguides at the input and output of a short section of multimode waveguide. The multimode waveguide region is designed so that its length coincides with one of the self-imaging planes at its output, so that, for example, each input waveguide is imaged onto one output waveguide. This self-imaging phenomenon which arises in multimode optical waveguides [10] can be used to image a small spotsize beam into the middle of a microfluidic channel. Figure 1 illustrates a conceptual microflow cytometry device with two MMIs arranged perpendicular to a microfluidic channel; one images the monomode waveguide mode profile into the microfluidic channel and the other collects light on the far side of the microfluidic channel.

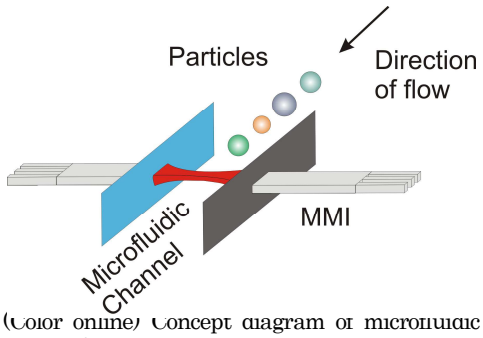

Fig. 1. (Color online) Concept diagram of microfluidic channel with integrated MMIs imaging to a spot in a microfluidic channel. Particles are either focused hydrodynamically or by dielectrophoresis and pass through the beam waist.

The advantages of using MMIs for focusing include simple design and layout, less stringent fabrication tolerances than for diffractive micro-lenses, allowing accurate replication by conventional photolithography, and two-dimensional confinement of the light up to the edge of the microfluidic channel resulting in reduced diffractive losses.

The length required for the multimode region in an imaging MMI is given by [10],

$$L = \frac{4 n_c W_e^{\,2}}{\lambda_0} + \delta \qquad (1)$$

where n_c is the effective refractive index of the core, W_e is the effective width of the multimode region resulting from evanescent penetration into the surrounding medium, λ_0 is the free-space wavelength, and δ is the offset length necessary for correction of the image plane due to the paraxial approximation [11]. Due to the Goos-Hähnchen shift, each mode in the multimode region will exhibit a different effective width, but for practical purposes the effective width is taken to be that for the fundamental mode and is given by [10],

$$W_e = W + \frac{\lambda_0}{\pi}\left(\frac{n_s}{n_c}\right)^{2\sigma}\left(n_c^{\,2} - n_s^{\,2}\right)^{-1/2} \qquad (2)$$

where σ is 0 for TE modes and 1 for TM modes and n_s is the effective refractive index of the surrounding material. Here we assume that the cores are clad with a medium of the same index as the substrate and n_s may be taken as the substrate index. Equation (1) gives the length required to replicate (image) the field at the input of the multimode region at its output, making no assumptions concerning which modes are excited in the MMI; this approach is known as general imaging. By exciting only selected modes, the required length can be reduced, and this is known as restricted self-imaging [10]. For instance, if only the symmetric modes are excited, the multimode region of an MMI can be made four times shorter.

Germania-doped silica waveguides on silica with $\Delta n \approx 0.016$ were chosen for compatibility with optical fibre. Since the required focal spot in the microfluidic channel should be Gaussian-like and as small as possible, single mode operation of the input channel waveguides is required. These waveguides were designed to have a width of 2 µm and a thickness of 1.9 µm. A physical MMI width of 22 µm was chosen to allow for three channel waveguide inputs spaced at 10 µm from the their centre, to avoid significant coupling between them.

The MMI was designed to ensure single mode operation in the vertical dimension (y-axis) throughout the device, including the multimode region. The effective refractive indices of the core regions were first determined to transform a 3D structure problem into a 2D structure problem. Simulations were then performed using the beam propagation method (BPM), which is computationally less complex and has lower memory requirements when reduced to two dimensions. Figure 2 shows an example BPM simulation, comprising a restricted-imaging MMI, imaging the input of the central input waveguide into the middle of a 20 µm microfluidic channel, with an identical MMI collecting the light. The central waveguide is excited and the MMI images this input into the middle of the microfluidic channel.

The first term of Eq. (1) is calculated as a starting point, but the offset length, δ, can only be found empirically or by numerical simulation. Simulations showed an optimum general self-imaging MMI length of 4988 µm with a δ of 40 µm and an optimum restricted self-imaging MMI length of 1247 µm with a δ of 10 µm. This agrees with the 4 times length reduction for symmetrical interference compared to the general imaging case.

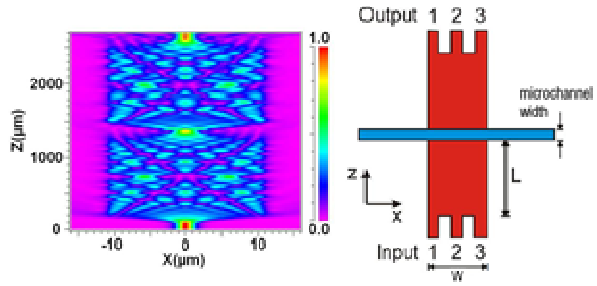

Fig. 2. (Color online) BPM simulation of restricted-imaging MMI, imaging the input of the central input waveguide into the middle of a 20 µm microfluidic channel.

The offset length, δ, is used to increase or decrease the length of the MMI to correct for the paraxial approximation of Eq. (1). In the case of imaging into a microfluidic channel, δ can be adjusted to place the focus of the beam further into the channel, according to design requirements. Simulations showed that a 1 µm decrease in δ causes an approximate 1 µm shift of the focus further out across the microfluidic channel.

MMI devices with a range of lengths, to allow for fabrication tolerances were realized on silica chips using standard planar fabrication processes. Fabrication errors in MMI width will shift the position of the focus according to Eqs 1 and 2, so that for this design a 0.1 µm error in W would result in a ~40 µm shift in focal position. A 1.9 µm thick film of SiO_2:GeO_2 (75:25 wt %) was RF sputtered onto a fused silica substrate. The SiO_2:GeO_2 film had a refractive index of 1.474 and the substrate 1.458, measured by prism coupling and ellipsometry at a wavelength of 633 nm. Photolithography was performed to pattern the waveguides and MMIs, and argon ion milling was used to etch the patterns to a depth of 1.9 µm into the film, as shown in Figure 3. Simple monomode channel waveguides, identical to the MMI input/output waveguides, were realized alongside the MMI structures for the purposes of comparison of propagation in the microfluidic channel.

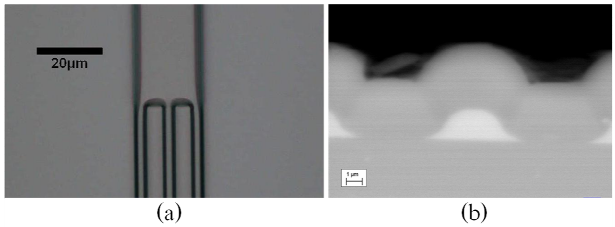

(a) (b)

Fig. 3. Images of input section of an MMI (a) optical microscope top-view before cladding and (b) SEM end view with cladding.

In the experimentally-realized devices, the channel waveguides are not rectangular but quasi-trapezoidal in cross-section. The widths of all the input and output monomode waveguides at the top and bottom were 2.6 µm and 5.3 µm, respectively, and they were separated by 10 µm from centre-to-centre. The top and bottom widths in the multimode region were 20.7 µm and 24.5 µm, respectively. A 4 µm thick cladding of silica was RF

sputtered on top of the etched waveguide cores. Conventional photolithography and Ar ion milling was then used to etch a microfluidic channel of depth 9 μm and width 100 μm through the centre of the multimode region of the MMIs, perpendicular to the waveguides. A microfluidic channel width of 100 μm was chosen to allow easier experimental determination of the focal position. BPM simulations show that widening the microfluidic channel to this extent does not significantly affect the focal position with respect to the center of the microfluidic channel. Finally, to seal the microfluidic channel a glass cover slip was attached on top. For the purposes of comparison, single mode waveguides crossing the same microfluidic channel were also included in the design.

The microfluidic channel was filled with an aqueous solution of Cy 5.5 fluorophore with a concentration of 50 μM, to allow visualization of light propagating across it. Light at a wavelength of 633 nm was coupled into a central input waveguide and fluorescence images were taken from above the chip using a microscope equipped with a CCD camera and a filter to remove 633 nm light but pass fluorescent light at wavelengths beyond 675 nm. Figure 4 shows fluorescent images taken for the beam from (a) a simple monomode channel waveguide crossing the microfluidic channel and (b) a general-imaging MMI of length L=4960 μm. Figures 4 (c) and (d) show these intensity data normalized to power at each cross-section (to eliminate the effects of absorption and scattering) with the dashed black line fit indicating the $1/e^2$ intensity contours acquired by fitting the equation for a Gaussian beam to the spotsizes measured along the beam. The spotsizes ($1/e^2$ intensity) themselves were found by fitting Gaussian curves to the intensity distribution in the x-axis.

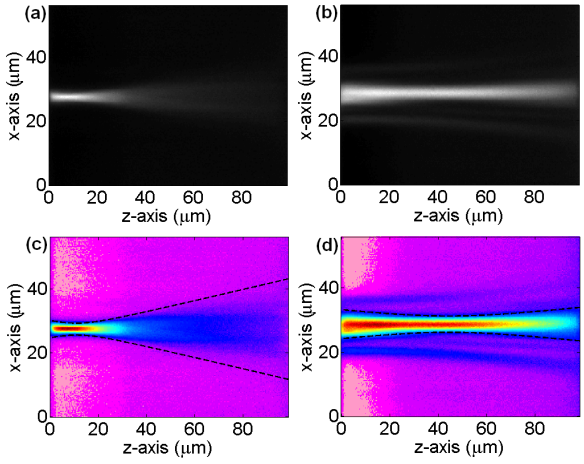

Fig. 4. (Color online) Fluorescent images of microfluidic channels for a channel waveguide (a) and an MMI (b) and Gaussian beam best fit (c) and (d), respectively.

In these images of the 100 μm wide microfluidic channel, the left hand side (z=0) represents one wall of the microfluidic channel while the right hand side (z=100 μm) represents the further wall of the microfluidic channel, so that only the light in the microfluidic channel is shown. The spotsize of the beam waist formed in the microfluidic channel for this MMI with L=4960 μm, was 2.4 μm and the position of the focus was 43.7 μm into the microfluidic channel. Thus the focal point was ~5004 μm from the beginning of the MMI, compared with the initial BPM design distance of 4998 μm (4988 μm to the channel wall), an error of 6 μm. This error is small considering the non-ideal cross-sections of the fabricated waveguides and the strong dependence of focal position on MMI width described by Equations 1 and 2. The waveguide modal spotsize along the y-axis is 1.6μm which, in an aqueous medium, will diffract in the y-direction to 2.5 μm over a 20 μm microfluidic channel width and to 9.7 μm over a 100 μm microfluidic channel. For comparison, the spotsize at the microfluidic channel wall of a channel waveguide mode emerging directly into the microfluidic channel was 2.5 ± 0.5 μm, and this mode diverged into the microfluidic channel so that it exhibited a spotsize of 9.4 ± 0.5 μm at a distance of 43.7 μm into the microfluidic channel, where the MMI formed its focus. The MMI clearly shows the ability to reimage the spot from the end of a channel waveguide at a distance into the microfluidic channel selected by MMI length. These MMIs are estimated to exhibit an excess loss of less than 0.2 dB, and inclusion of an MMI in a cytometer chip, replacing a short length of waveguide between the chip edge and the microfluidic channel, is not expected to increase insertion loss measurably.

In conclusion, the multimode interference device (MMI) has been presented as an alternative to the micro-lens for use in the lab-on-a-chip, showing good performance in imaging a spot in a microfluidic channel for microflow cytometry. The design was initiated using simple theoretical expressions and then optimized by BPM simulation. MMIs were realized in a silica glass material system and characterized to show imaging of a spot into the microfluidic channel. These devices pave the way to the full integration of more robust and complex microfluidic microflow cytometers.

The authors would like to thank Dr. P. Hua for preparation of the fluorescent media and Dr. D. Gallagher of Photon Design for advice on MMIs.

References

1. A. Ateya, J. S. Erickson, P. B. Howell Jr, L. R. Hilliard, J. P. Golden, and F. S. Ligler, Anal. Bioanal. Chem. **391**, 1485 (2008).
2. H. C. Hunt and J. S. Wilkinson, Microfluid. Nanofluid. **4**, 53 (2008).
3. C. Dongre, J. van Weerd, G. A. J. Besselink, R. van Weeghel, R. M. Vazquez, R. Osellame, G. Cerullo, M. Cretich, M. Chiari, H. J. W. M. Hoekstra, and M. Pollnau, Electrophoresis **31**, 2584 (2010).
4. S. Camou, H. Fujita, and T. Fujii, Lab Chip **3**, 40 (2003).
5. J. Seo and L. P. Lee, Sens. Actuators B **99**, 615 (2004).
6. J. Godin, V. Lien, and Y-H. Lo, Appl. Phys. Lett. **89**, 061106 (2006).
7. V. Moreno, J. Roman, and J. Salgueiro, Am. J. Phys. **65**, 556 (1997).
8. H. C. Hunt and J. S. Wilkinson, Photon10, Southampton, UK, 23-26 Aug 2010.
9. H. C. Hunt and J. S. Wilkinson, MOC09 (15th Micro-optics Conference), Odaiba, Japan, 25-28 Oct, 2009, J14.
10. L. B. Soldano and E. C. M. Pennings, J. Lightwave Technol. **13**, 615 (1995).
11. K. Okamoto, *Fundamentals of Optical Waveguides*, 2nd ed. (Academic Press, 2006)

FULL REFERENCES

1. A. Ateya, J. Erickson, P. Howell, L. Hilliard, J. Golden, and F. Ligler, "The good, the bad, and the tiny: a review of microflow cytometry," Analytical and Bioanalytical Chemistry, vol. 391, no. 5, pp. 1485-1498, 2008.

2. H. C. Hunt and J. S. Wilkinson, "Optofluidic integration for microanalysis," Microfluidics and Nanofluidics. 4(1-2): 53-79, 2008.

3. C. Dongre, J. van Weerd, G.A.J. Besselink, R. van Weeghel, R.M. Vazquez, R. Osellame, G. Cerullo, M. Cretich, M. Chiari, H.J.W.M. Hoekstra, and M. Pollnau, "High-resolution electrophoretic separation and integrated-waveguide excitation of fluorescent DNA molecules in a lab on a chip" Electrophoresis, 31, no 15, 2584-2588, 2010.

4. S. Camou, H. Fujita, and T. Fujii, "PDMS 2D optical lens integrated with microfluidic channels: principle and characterization," Lab on a Chip, vol. 3, no. 1, pp. 40-45, 2003.

5. J. Seo and L. Lee, "Disposable integrated microfluidics with self-aligned planar microlenses," Sensors and Actuators B-Chemical, vol. 99, no. 2-3, pp. 615-622, 2004.

6. J. Godin, V. Lien, and Y. Lo, "Demonstration of two-dimensional fluidic lens for integration into microfluidic flow cytometers," Applied Physics Letters, vol. 89, no. 6, p. 061106, 2006.

7. V. Moreno, J. Roman, and J. Salgueiro, "High efficiency diffractive lenses: Deduction of kinoform profile," American Journal of Physics, vol. 65, no. 6, pp. 556-562, 1997.

8. H. C. Hunt and J. S. Wilkinson, "Microlenses for flow cytometry," Photon10, Southampton, 23-26 Aug 2010.

9. H. C. Hunt and J. S. Wilkinson, "Integrated lenses for microfluidic systems," MOC09 (15th Micro-optics Conference), Odaiba, Japan, 25-28 Oct, 2009, J14.

10. L. B. Soldano and E. C. M. Pennings, "Optical multimode interference devices based on self-imaging - principles and applications," Journal of Lightwave Technology, vol. 13, no. 4, pp. 615-627, 1995.

11. K. Okamoto, Fundamentals of Optical Waveguides, 2nd ed. Academic Press, 2006